

MILITARY TECHNICAL COLLEGE  
CAIRO - EGYPT



7<sup>th</sup> INTERNATIONAL CONF. ON  
AEROSPACE SCIENCES &  
AVIATION TECHNOLOGY

## Effect of Fe Codeposition with Zn-Ni on Crystal Structure and Microhardness in Comparison with Zn-Ni Alone

Ibrahium Hamed M. ALY\*, O. A. FADALI\*, M. M. YOUNAN\*\*,  
M. A. ARAFA\*\*\*, A. T. EL-MALLAH\*\*\* and T. OKI\*\*\*\*

### ABSTRACT

Bath compositions for electrodeposition of Zn-Ni-Fe in chloride baths were studied. Varying concentration of metal ions in the bath were used, at constant operating conditions, to obtain alloys containing 14 to 20 % nickel and up to 7.25% iron. It was found that the nickel content in the deposits not affected by addition of ferrous chloride from 0.02 to 0.08 M to the plating bath. The codeposits without iron showed  $\gamma$  phase structure with preferred crystal orientation (330) and (411). However, the crystal orientation of  $\gamma$  phase changed to prefer (442) and (600) with iron codeposited in the Zn-Ni alloy. The microhardness of the deposits increases were observed, in these experiments, with increasing of iron content in the deposits. The highest hardness (535 VHN) found from the deposit obtained in the bath containing 0.5/0.4  $\text{Ni}^{2+}/\text{Zn}^{2+}$  molar ratio with addition 0.04 mol/l  $\text{Fe}^{2+}$ .

### KEY WORDS

[Zn-Ni electrodeposition, Separated anodes, Fe codeposition, Crystal Structure, Microhardness.]

[\* Professor, Dpt. of Chemical Engineering, Faculty of Engineering, El-Minia University, Egypt. \*\* Graduate student, Dpt. of Chemical Engineering and Pilot Plant, National Research Centre, Giza, Egypt. \*\*\* Professor, Dpt. of Chemical Engineering and Pilot Plant, National Research Centre, Giza, Egypt. \*\*\*\* Professor, Dpt. of Materials Science and Engineering, Faculty of Engineering, Nagoya University, Japan.]

## 1. INTRODUCTION

Many efforts have been made to develop high corrosion resistance steel sheets, especially, for automotive body panels [1-4]. Recently, it has been shown that electrodeposited zinc-iron group metal alloys are suitable materials for this application [1-8]. A major development in this area has been directed toward zinc-nickel (8-20%) alloy coatings because of higher degree of corrosion resistance and better mechanical properties than a pure zinc layer [7-9].

Most of the recent papers cited in the scientific and marketing literature dealing with improved zinc electroplating studies and application performed by Japanese authors [1,4]. Many papers are concerned with patents in the electrodeposition of binary Zn-Ni alloy coatings and therefore no information on the electrodeposition of ternary Zn-Ni-Fe alloy coatings.

In the present work, binary Zn-Ni and ternary Zn-Ni-Fe alloy coatings were obtained on mild steel by electroplating in a chloride bath. In order to make a clear comparison between Zn-Ni and Zn-Ni-Fe alloys for microhardness and crystal structure, the ternary deposits were obtained at similar operating conditions to the binary alloy.

## 2. EXPERIMENTAL PROCEDURE

All plating baths were freshly prepared from distilled water and analytical grade reagents. The basic bath components required for electrodeposition of Zn-Ni deposits, are listed in Table 1, also, Zn-Ni-Fe alloy electrodeposited from the same one with adding ferrous chloride (0.02 to 0.08 M) to the solution. All the prepared deposits were obtained at temperature of  $43 \pm 2$  °C, current density of  $30 \text{ mAcm}^{-2}$  and pH of 3, in 10 minutes electroplating.

The experimental setup for the electrodeposition process consisted of a rectangular glass cell containing  $200 \text{ cm}^3$  of electrolyte solution and proper electric circuit. Electrodeposits were electroplated on one side of mild steel plate of 1 mm thickness (exposed area  $9 \text{ cm}^2$ ). Before electrodeposition, the steel substrates were pretreated as following; degreasing by organic solvent (acetone), water rinsing, alkaline soaking in 6% NaOH solution, water rinsing, acid neutralization and activation in 10% HCl solution and finally rinsing with distilled water. Then, the samples were used for plating.

For electrodeposition of ternary Zn-Ni-Fe alloy, the anode electrodes consist of a zinc ( $7.2 \text{ cm}^2$ ), a nickel ( $1.2 \text{ cm}^2$ ) and an iron ( $0.6 \text{ cm}^2$ ) sheets. The each anodic electrodisso-

was regulated separately by three independent circuits, by which, zinc, nickel and iron consumption in electrolyte due to their reduction at cathode was compensated

**Table 1.** The basic bath composition for electrodeposition of ternary Zn-Ni-Fe alloy.

Bath Ingredient	Concentration, mol/l
Zinc chloride ( $\text{ZnCl}_2$ )	0.40
Nickel chloride ( $\text{NiCl}_2 \cdot 6\text{H}_2\text{O}$ )	0.40
Sodium chloride ( $\text{NaCl}$ )	2.50
Sodium acetate ( $\text{CH}_3\text{COONa} \cdot 3\text{H}_2\text{O}$ )	0.30
Boric acid ( $\text{H}_3\text{BO}_3$ )	0.50
Dodecyl sodium sulfate, (wetting agent)	0.50*

\* This concentration was in g/l.

The experiments for determining the deposit composition and the crystal structure were carried out by using copper substrate, and the substrate for measurement of hardness and grain size was mild steel as usual. To determine the deposit composition, the deposits were stripped in 10% HCl solution and then analyzed as for Fe and Ni by means of atomic absorption.

The microhardness of deposits was measured by micro-Vickers pyramidal indenter with 25 g load and each value is the average of seven measurements at least. The crystal orientation was characterized by X-ray diffraction method by  $\text{CuK}\alpha$  ( $\lambda = 1.54 \text{ \AA}$ ). The grain size of the alloy coatings was examined by using scanning electron microscopy (SEM). Before SEM examination, the samples were etched in 10% HCl solution to make the determination of grain size clear.

### 3. RESULTS AND DISCUSSION

#### 3.1) Chemical Composition of The Deposit

The relationship between deposit composition and both  $\text{ZnCl}_2$  and  $\text{NiCl}_2$  concentrations in the bath for the binary Zn-Ni alloys are shown as the case of no  $\text{FeCl}_2$  in Figs. 1 and 2. It can be seen in this figures that the zinc is the most readily deposited metal and alloy deposition is of the anomalous type [8,10].

Figures 1 and 2, also, illustrated the influence of ferrous chloride concentration on the deposit composition of ternary Zn-Ni-Fe alloy coatings. The nickel content in the alloys was approximately constant in spite of ferrous chloride addition. However, the iron content in the films increased with increasing ferrous ions in the bath. Also, it was observed that the iron content in the deposited alloy was increased with increasing nickel ions concentration in the bath. For example, the iron content in deposits was changed to 1.50%, 3.95% and 5.80%, respectively by different molar ratios of 0.4/0.6, 0.4/0.4 and 0.5/0.4 of  $\text{Ni}^{2+}/\text{Zn}^{2+}$  in electrolyte with 0.06 M  $\text{Fe}^{2+}$ . The increase in deposit iron content corresponds with increasing  $\text{Ni}^{2+}/\text{Zn}^{2+}$  molar ratio. This may be attributed to the decrease in the overpotential of iron deposition due to the increasing  $\text{Ni}^{2+}/\text{Zn}^{2+}$  molar ratio in bath.

### 3.2) Crystal Orientation of Films

The X-ray diffraction patterns of Zn-Ni-Fe films as a function of Fe content are shown in Figs. 3 - 6. Only the  $\gamma$  phase is present in zinc-nickel coatings with above 8-9% Ni; the thing which is consistent in previous papers [11,12]. Zinc-nickel alloys with 14.17 to 19.25% Ni were found to be formed of the single  $\gamma$  phase, which agrees with the zinc-nickel equilibrium diagram as already noted by some authors[3,13,14]. From case (a) without Fe in Figs. 3 to 6, the  $\gamma$  phase showed a preferential (330) and (411) crystal orientation, what was confirmed by Shibuya et al.[3].

Under the same electroplating conditions, the crystal orientation of  $\gamma$  phase in the Zn-Ni-Fe deposits was found to depend on the iron content in it. From Fig. 4, as example for Zn-Ni-Fe deposits, it can be seen that the  $\gamma$  phase showed a clear change to prefer (442) and (600) crystal orientation. This orientation was due to codeposition of iron causing a change of crystal growth of the deposited zinc-nickel alloy. The same trend of the crystal orientation was observed for different deposits, as shown in Figs. 3, 5, and 6.

The change of this preferred crystal orientation may be explained considerably good by the adsorption inhibition theory according to Wang and Oki [15]. This theory for this phenomena is as follows; some Fe atoms adsorb on active plane or sites, which have relative high energy, and inhibit crystal growth reaction on that plane or spot. The growing direction of crystals is changed by this inhibition. The remaining plane becomes a preferred oriented one. Then through this mechanism, the preferred orientation changed to another direction.

In these experiments, as there are no organic additives in the plating baths, iron acts as an inhibitor. The  $\gamma$  phase grows in the direction of  $\langle 442 \rangle$ ,  $\langle 600 \rangle$  or  $\langle 444 \rangle$  better than that of  $\langle 411 \rangle$  or  $\langle 330 \rangle$  in baths without iron and the remaining plane is (411) or (330). As for the

behavior in baths with iron, the iron adsorbs and codeposits on (442), (600) and (444) and inhibit crystal growth in the direction of <442>, <600> and <444>. Consequently, the relative intensity of (411), (330) decreases and these of (442), (600) and (444) increase with increasing of iron content in the deposits, as shown in Figs. 3 to 6.

Moreover the confirmation for action of Fe codeposition as inhibitor, it was found that the position of peaks in  $2\theta$  (in X-ray chart) is slightly shifted to smaller angle with iron codeposition, as shown in Fig. 7. This means that the crystal lattice spaces ( $d$ ) are increased by codeposition of iron into the lattice of Zn-Ni. Also, the grain size of the Zn-Ni-Fe deposits became very fine and more homogeneous in comparison with those of binary Zn-Ni deposits.

### 3.3) The Microhardness Measurement

It was known that the microhardness of electrodeposited Zn-Ni alloy coatings was increased with increasing Ni content as already studied by Felloni *et al.* [11] and by other authors [7,14,16]. Moreover the increase in microhardness was observed, in the present work, when iron codeposited with Zn-Ni alloy to form ternary Zn-Ni-Fe alloy coatings.

The measured microhardness values of the deposits were plotted as a function of iron content, as illustrated in figs. 8 and 9. From these figures, it can be seen the real increase in the microhardness with increasing of iron content in the deposits containing approximately same nickel content. This relation is satisfied at various values of iron content also in the deposits having different nickel content.

In this work, there appears to be a strong relation between microhardness and iron codeposition. When the alloy nickel content was constant, the microhardness increased with increasing the iron content in the alloy up to a certain value, as shown in Figs. 8 to 9. Therefore, many attempts have been made to correlate the alloy composition with microhardness for Zn-Ni and Zn-Ni-Fe electro-deposits. The best correlation was found to relate the increase in microhardness ( $VHN_{Zn-Ni-Fe} - VHN_{Zn-Ni}$ ) with  $[Fe \times 100 / Zn (Fe + Ni)]\%$  in a linear relationship, as shown in Fig. 10, according to the following equation:

$$VHN_{Zn-Ni-Fe} - VHN_{Zn-Ni} = 1.7662 + 7.3034 \left( \frac{Fe \times 100}{(Fe + Ni)Zn} \right) \%$$

Where:

$VHN_{Zn-Ni-Fe}$  : microhardness of Zn-Ni-Fe deposits, kg/mm<sup>2</sup>,

$VHN_{Zn-Ni}$  : microhardness of Zn-Ni deposits, kg/mm<sup>2</sup>, and

Fe, Ni and Zn : the percentage of iron, nickel and zinc in deposits, wt%.

This above equation is valid only when the binary and ternary deposits containing approximately the same nickel content and up to the term  $\left( \frac{\text{Fe} \times 100}{(\text{Fe} + \text{Ni})\text{Zn}} \right) \%$  equal about 24.

In general, three factors seemed to influence the deposit microhardness [17]; the fineness of the grain, the dislocation density and the pinning of the dislocations by impurities. The deposits with the smaller grain size and the higher strains tend to give higher hardness value. The increase in the microhardness of Zn-Ni-Fe alloys deposits with increasing iron content agreed with the effect of iron content due to the fineness of grain size and the change of lattice space which showed the strain in the film as explained previously. Therefore, the increases in hardness of Zn-Ni-Fe deposits are attributed not only to the increase of nickel content in the alloy as found for Zn-Ni deposits but also more fine grain size and  $\delta$  distortion in the lattice of the deposited alloy due to iron codeposition as already observed.

#### 4. CONCLUSION

The electrodeposition of Zn-Ni-Fe alloys from the acidic chloride electrolyte exhibited the phenomenon of anomalous codeposition. The iron content in Zn-Ni-Fe deposits is increased with increasing of  $\text{Ni}^{2+}/\text{Zn}^{2+}$  molar ratio in the baths with the same  $\text{FeCl}_2$  concentration.

The  $\gamma$  phase of the Zn-Ni deposits only (14.17 to 19.25% Ni) showed a preferential (411) and (330) crystal orientation. When iron codeposited into the deposits, the  $\gamma$  phase showed a clear change to prefer (442), (600) or (444) crystal orientation. Also, the crystal lattice spaces are increased by codeposition of iron into the lattice of Zn-Ni up to 4 wt.% Fe content.

The microhardness of the thin films was increased with increasing of iron content even in the deposits containing approximately the same nickel content. The highest hardness (535 VHN) obtained from the deposit produced from the bath containing 0.5/0.4  $\text{Ni}^{2+}/\text{Zn}^{2+}$  molar ratio with addition 0.04 mol/l  $\text{Fe}^{2+}$ .

#### REFERENCES

- [1] T. Watanabe *et al.*, SAE Tech. Pap. Series No 820424, Detroit, Michigan (1982).
- [2] A. Shibuya *et al.*, *Tetsu to Hagane* **66** (1980) 771.
- [3] R. Noumi *et al.*, SAE Tech. Pap. Series No 820332, Detroit, Michigan (1982).



- [4] T. Kurimoto *et al.*, SAE Tech. Pap. Series No 831837, Warrendale, Pennsylvania (1983).
- [5] K. Ariga and K. Kanda, *Tetsu to Hagane*, **66** (1980) 797.
- [6] T. Fukuzuka, K. Jajiawara and K. Miki, *Tetsu to Hagane*, **66** (1980) 807.
- [7] V. Raman *et al.*, *Met. Finish.*, **81** (1983) 85.
- [8] D. E. Hall, *plat. surf. Finish.*, **71** (1983) 59.
- [9] G. F. Hsu, *plat. surf. Finish.*, **72** (1984) 52.
- [10] A. Brenner, "Electrodeposition of Alloys" Vol. 1, Academic Press, New York and London (1963).
- [11] L. Felloni *et al.*, *J. Appl. Electrochem.*, **17** (1987) 574.
- [12] L. Felloni *et al.*, *Proceedings of XXII International Metal Congress*, Bologna, Italy, (17-19 May 1988) P. 687.
- [13] T. L. Rama Char and S. K. Panikker, *Electroplat. Met. Finish.*, **13** (1960) 405.
- [14] M. R. Lambert *et al.*, SAE Tech. Pap. Series No 831817, Detroit, Michigan (1983).
- [15] D. D. Wang and T. Oki, *J. Vac. Sci. Technol. A.*, **8** (1990) 3163.
- [16] H. Tsuji and M. Kamitani, Proc. AES 69th Annual Conference, Paper P2 (20-24 June, 1982).
- [17] R. Walker and R. C. Benn, *Plating*, **69** (1977) 476.

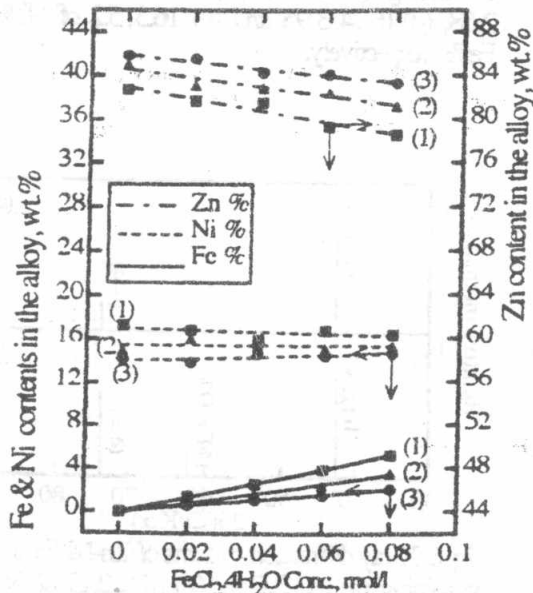


Fig. 1. Effect of ferrous chloride concentration in the bath on electrodeposited Zn-Ni-Fe alloy composition from baths containing (1) 0.4, (2) 0.5 and (3) 0.6 mol/l  $\text{ZnCl}_2$ .

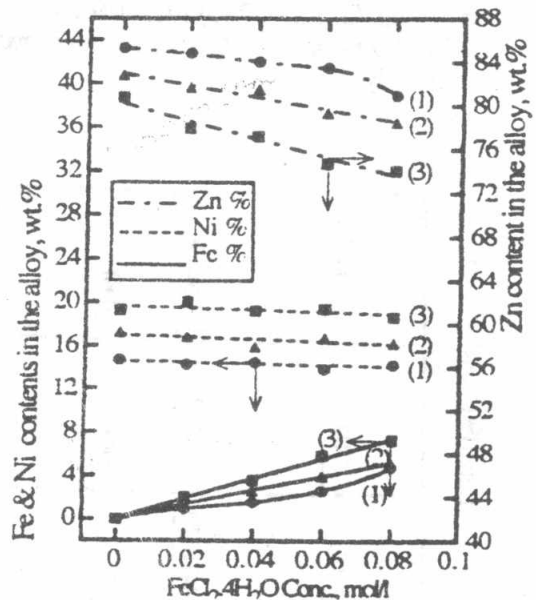


Fig. 2. Effect of ferrous chloride concentration in the bath on electrodeposited Zn-Ni-Fe alloy composition from baths containing (1) 0.3, (2) 0.4 and (3) 0.5 mol/l  $\text{NiCl}_2$ .

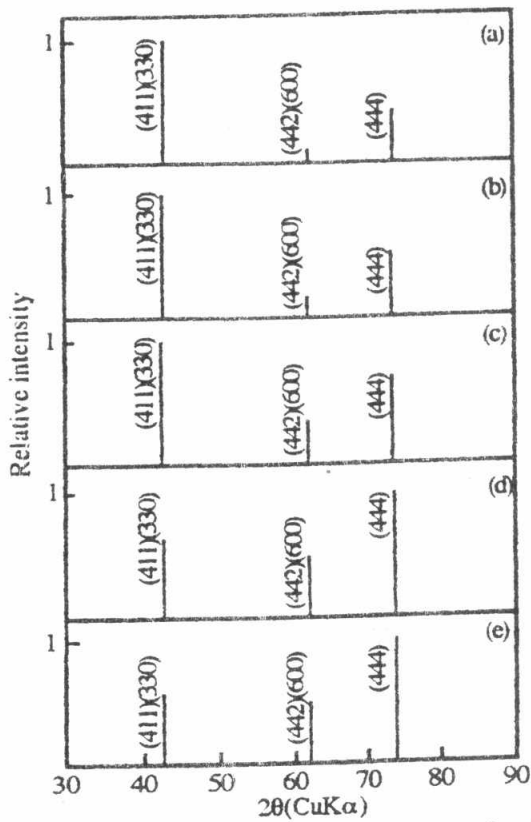


Fig. 3. X-ray diffraction patterns of Zn-Ni-Fe alloy films containing: (a) 14.74, 0, (b) 14.29, 0.93, (c) 14.46, 1.5, (d) 13.92, 2.64 and (e) 14.28, 4.74 of Ni% and Fe%, respectively.

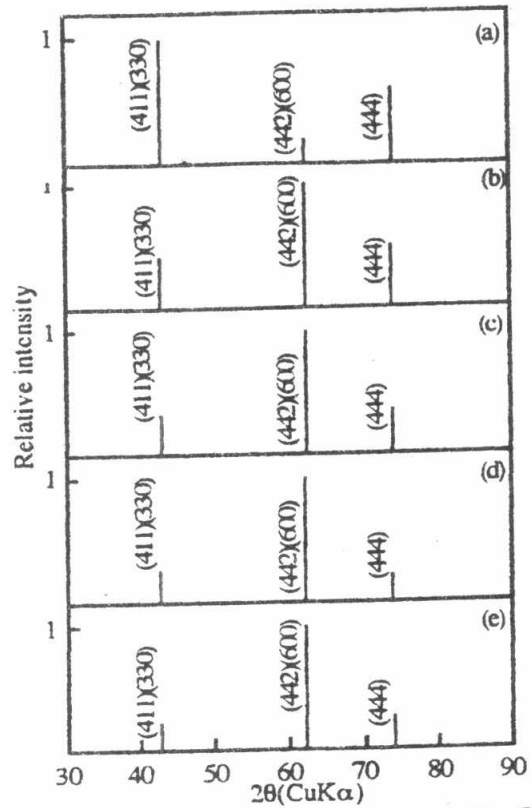


Fig. 4. X-ray diffraction patterns of Zn-Ni-Fe alloy films containing: (a) 17.26, 0, (b) 16.84, 1.47, (c) 15.91, 2.58, (d) 16.74, 3.95 and (e) 16.3, 5.2 of Ni% and Fe%, respectively.

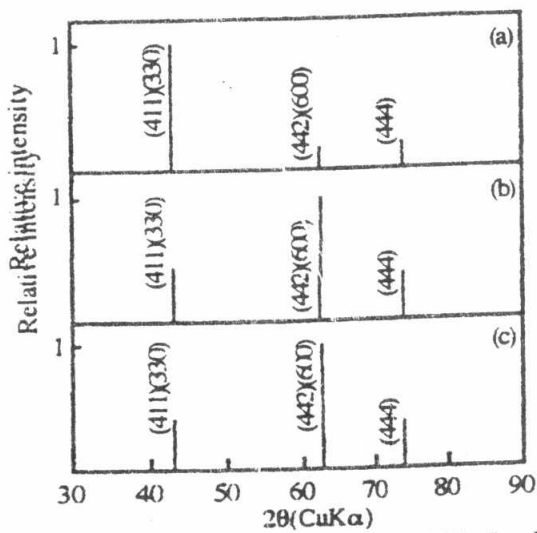


Fig. 5. X-ray diffraction patterns of Zn-Ni-Fe alloy films containing: (a) 19.25, 0, (b) 19.23, 3.61 and (c) 18.67, 7.25 of Ni% and Fe%, respectively.

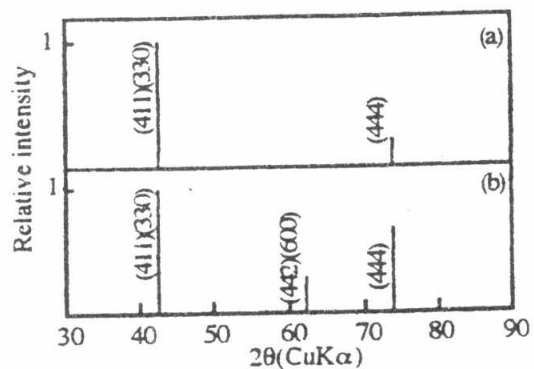


Fig. 6. X-ray diffraction patterns of Zn-Ni-Fe alloy films containing: (a) 14.17, 0 and (b) 14.6, 2.13 of Ni% and Fe% respectively.



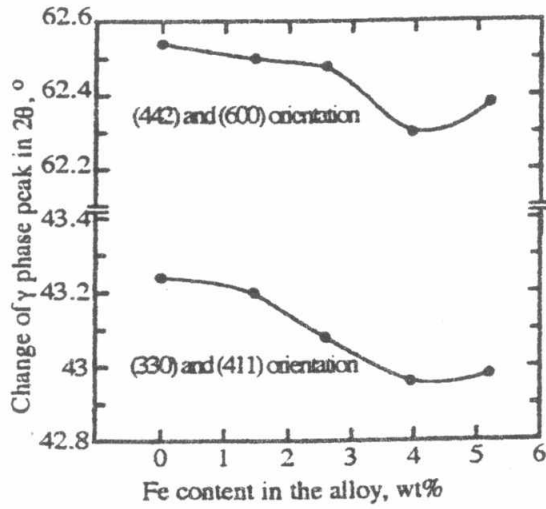


Fig. 7. Influence of Fe codeposition on the position of  $\gamma$  in  $2\theta$  for Zn-Ni-Fe plated from the bath containing 0.4 mol/l of Ni and Zn ions.

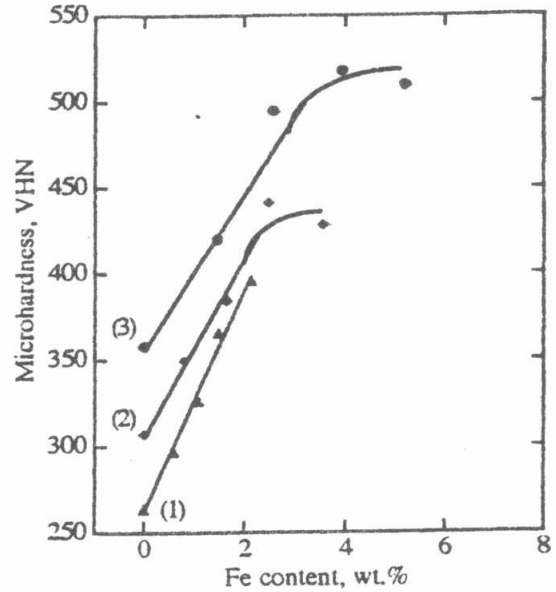


Fig. 8. Microhardness Vs. Fe content for the alloys electrodeposited in baths containing: (1) 0.6, (2) 0.5 and (3) 0.4 mol/l  $ZnCl_2$ .

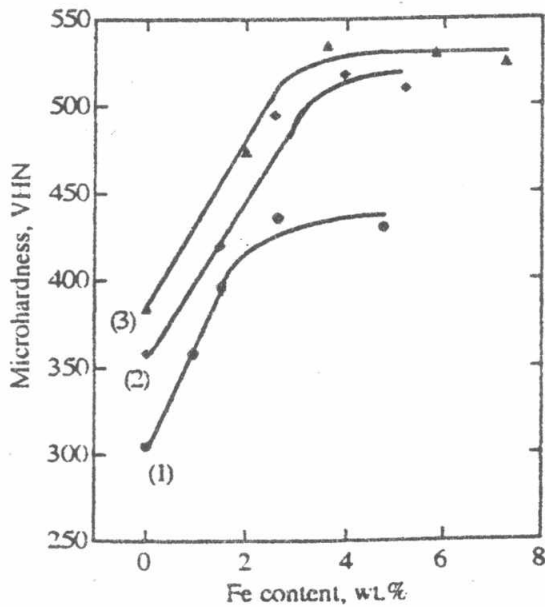


Fig. 9. Microhardness Vs. Fe content for the alloys electrodeposited in baths containing: (1) 0.3, (2) 0.4 and (3) 0.5 mol/l  $NiCl_2$ .

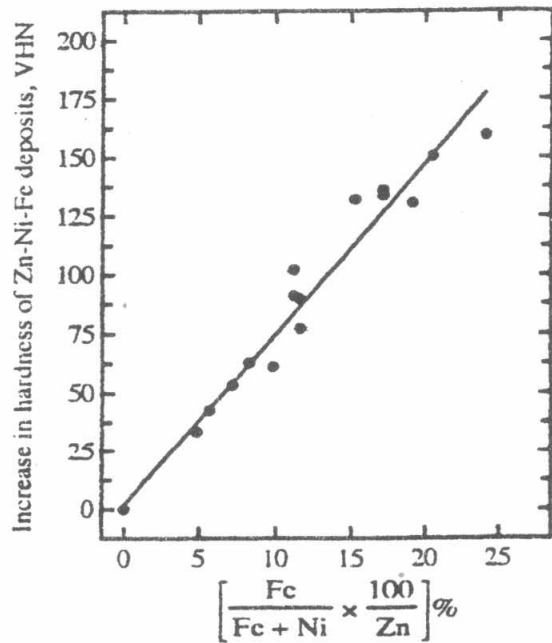


Fig. 10. The relation between the increase in microhardness of Zn-Ni-Fe deposits and  $\left[ \frac{Fe}{Fe + Ni} \times \frac{100}{Zn} \right] \%$ .